Авторлар туралы мәліметтер

Меруертқожа Тоқтарбек* – PhD, «Органикалық заттар, табиғи қосылыстар және полимерлер химиясы мен технологиясы» кафедрасының аға оқытушысы; әл-Фараби атындағы Қазақ ұлттық университеті, Алматы, Қазақстан; e-mail: meruyertkozha@mail.ru. ORCID: https://orcid.org/0000-0002-0979-6944.

Карина Сарахмет – «Химия және химиялық технология» факультетінің бакалавры; әл-Фараби атындағы Қазақ ұлттық университеті, Алматы, Қазақстан; e-mail: sarahmet04@mail.ru.

Гаухар Шахманқызы Бурашева – химия ғылымдарының докторы, «Органикалық заттар, табиғи қосылыстар және полимерлер химиясы мен технологиясы» кафедрасының профессоры; әл-Фараби атындағы Қазақ ұлттық университеті, Алматы, Қазақстан; e-mail: gauharbur@mail.ru. ORCID: https://orcid.org/0000-0003-2935-3531.

Балақыз Қымызғалиқызы Есқалиева – химия ғылымдарының кандидаты, «Органикалық заттар, табиғи қосылыстар және полимерлер химиясы мен технологиясы» кафедрасының қауым. профессоры; e-mail: balakyz@mail.ru. ORCID: https://orcid.org/0000-0002-1745-2738.

Өзтүрк Мехмет – PhD, Мугла Ситка Кочман университеті, ғылым факультеті, химия кафедрасының профессоры, Мугла, Түркия; e-mail: mehmetozturk@mu.edu.tr. ORCID: https://orcid.org/0000-0001-8932-4535.

Сведения об авторах

Меруерткожа Токтарбек* – PhD, старший преподаватель кафедры «Химия и технология органических веществ, природных соединений и полимеров»; Казахский национальный университет имени аль-Фараби, Алматы, Казахстан; e-mail: meruyertkozha@mail.ru. ORCID: https://orcid.org/0000-0002-0979-6944.

Карина Сарахмет – Бакалавр факультета «Химия и химическая технология»; Казахский национальный университет имени аль-Фараби, Алматы, Казахстан; e-mail: sarakhmet04@mail.ru.

Гаухар Шахмановна Бурашева – доктор химических наук, профессор кафедры «Химия и технология органических веществ, природных соединений и полимеров»; Казахский национальный университет имени аль-Фараби, Алматы, Казахстан; e-mail: gauharbur@mail.ru. ORCID: https://orcid.org/0000-0003-2935-3531.

Балакыз Кымызгалиевна Ескалиева – кандидат химических наук, ассоц. профессор кафедры «Химия и технология органических веществ, природных соединений и полимеров»; Казахский национальный университет имени аль-Фараби, Алматы, Казахстан; e-mail: balakyz@mail.ru. ORCID: https://orcid.org/0000-0002-1745-2738.

Озтюрк Мехмет – PhD, профессор кафедры химии, факультета науки, Университета Мугла Ситки Кочман, Мугла, Турция; e-mail: mehmetozturk@mu.edu.tr. ORCID: https://orcid.org/0000-0001-8932-4535.

Received 14.08.2024
Revised 23.09.2024
Accepted 24.09.2024

https://doi.org/10.53360/2788-7995-2024-4(16)-44

IRSTI: 31.15.29

N. Maksut[1], B. Tatykayev[2], S. Tugelbay[2], A. Abilkhan[2], N. Khan[2*]

[1]Al-Farabi Kazakh National University,
050040, Kazakhstan, Almaty, Al-Farabi Ave. 71
[2]Nazarbayev University,
010000, Kazakhstan, Astana, Kabanbay batyr av. 53
*email: natalya.khan@nu.edu.kz

COMPARATIVE STUDY OF PHOTOCATALYTIC HYDROGEN EVOLUTION ON G-C_3N_4 DECORATED WITH NIS AND NIS_2 CO-CATALYSTS VIA ION EXCHANGE PRECIPITATION METHOD

Abstract: *NiS and NiS_2 co-catalysts were decorated on the surface of g-C_3N_4 through ion exchange reaction by precipitation method. Synthesized double systems were investigated using XRD, FT-IR, SEM, TEM, and TEM elemental mapping. XRD and FT-IR analyses showed the presence of g-C_3N_4 in the composition of g-C_3N_4/NiS and g-C_3N_4/NiS_2, however the presence of nickel sulfides was not identified. SEM analysis showed that double systems have heterogeneous systems, the stacked flat sheets with wrinkles and an irregular shape morphology and rough surface, where the presence of irregular shape pores is visible. TEM proved the presence of irregularly*

shaped layers of g-C_3N_4, and TEM elemental mapping showed the presence of nitrogen, carbon, sulfur, and nickel. The ability of the photocatalytic hydrogen evolution by prepared samples revealed, that g-C_3N_4/NiS_2 manifests the highest hydrogen evolution rate in comparison with g-C_3N_4/NiS and g-C_3N_4. Thus, the highest evolution rate of hydrogen was reached by g-C_3N_4/NiS_2 on the 3rd hour of the visible light irradiation and was equal to 56.79 μmol$h^{-1}g^{-1}$.

Key words: *graphitic carbon nitride, nickel sulfide, co-catalyst, photocatalyst, hydrogen evolution.*

Introduction

Environmental problems and the global energy crises are becoming severe risks to the long-term advancement of human society [1]. In comparison with fossil fuels, hydrogen is less prevalent in nature. However, it may be created using any primary energy source and utilized as fuel for fuel cells or for direct combustion in internal combustion engines, simply emitting water as a byproduct [2]. There are many different methods for producing hydrogen (H_2) that, depending on the raw materials used, can be grouped into two main groups, namely conventional and renewable technologies [3]. The pyrolysis and hydrocarbon reforming processes are included in the first category, which deals with processing fossil fuels. Steam reforming, partial oxidation, and autothermal steam reforming are the chemical processes that take part in the hydrocarbon reforming process [4]. The second group includes processes that create hydrogen using biomass or water as renewable resources [5]. The second category of renewable technologies focuses on techniques that may produce H_2 gas from water using only water as an input, such as electrolysis, thermolysis, and photo-electrolysis [6].

One of the most promising methods to address energy and environmental issues is the photocatalytic hydrogen evolution reaction [7]. Since Fujishima and Honda first reported photoelectrochemical water splitting on a (titanium dioxide) TiO_2 electrode in 1972, photocatalytic water splitting for H_2 production has emerged as a promising method for the efficient, affordable, and environmentally friendly production of H_2 using solar energy [8]. The creation of effective, stable, and environmentally friendly photocatalysts is necessary for the manufacturing of practical solar fuels and, more generally, the conversion of solar energy into useful chemical products [9, 10]. The splitting of water occurs in photo-electrolysis when sunlight is absorbed through certain semiconducting materials. In particular, an electron-hole pair is produced and separated by the electric field between the semiconductor and the electrolyte if a photon with energy larger than or equal to the semiconductor's band gap reaches the semiconducting surface of the anode. Long-lived charge carriers, fewer charge trapping centers, the right energy level offsets, and stability against light are all extremely desirable for enhancing the photocatalytic reactivity of a semiconductor photocatalyst. Ideally, photocatalysts should have properties such as a good band gap, good band-edge potentials, high surface areas, and delayed charge recombination [11]. For such purposes, the photocatalytic performance of semiconductor photocatalysts has been improved during the past ten years using a variety of techniques, such as surface sensitization, interfacial heterostructures, band gap engineering, and crystal and textural alteration [2].

The metal-free graphite-like carbon nitride (g-C_3N_4) has gained mass attention since the first discovery of photocatalytic activity of material in 2008 by Wang's group [12]. Due to its broad light absorption range, structural stability, and low cost, the metal-free semiconductor g-C_3N_4 is a promising candidate for H_2 production because the photocatalyst contains earth-rich materials, which can enhance large-scale industrial application of H_2 generation [11, 13]. However, the practical and widespread use of g-C_3N_4 is typically constrained by its poor visible-light absorption, rapid charge recombination, and limited specific surface area [14]. Thus, numerous modifications such as using defect engineering [15] and constructing nano-scale structures [16] have been suggested to improve the photocatalytic potential of g-C_3N_4 by addressing these issues. Despite these modifications, the g-C_3N_4 is still incapable of achieving higher conversion rates due to insufficient surface catalytic sites. In addition, g-C_3N_4 has low charge mobility, resulting in the rapid recombination of electrons and holes. These factors diminish its photocatalytic efficiency, highlighting the need for its modification [11].

One approach to addressing the limitations of g-C_3N_4 is the use of co-catalysts, which enhance charge separation and reduce the recombination of electrons and holes. Additionally, co-catalysts facilitate more efficient electron transfer from the photocatalyst to the reagent molecules

involved in the photocatalytic process, thereby speeding up the reaction. Additionally, co-catalysts can form extra active sites, thereby enhancing the photocatalyst's overall activity [17]. Although noble metals like Pt, Ag, Au, and Pd [18] are the most commonly used co-catalysts, their high-cost limits widespread application [19]. As a result, increasing attention is being given to metal sulfides as alternatives to noble metals. For instance, copper sulfide (CuS) and molybdenum sulfide (MoS_2) exhibit high activity in photocatalytic H_2 production [20, 21]. Nickel sulfide (Ni_xS_y) is another promising material known for its high activity, stability, and durability [19, 20]. Nickel sulfide is able to greatly enhance the photocatalytic performance due to the synergistic effect when combined with carbon nitride.

In this regard, this study is devoted to the production of g-C_3N_4/NiS and g-C_3N_4/NiS_2 by precipitation method, which was used for photocatalytic hydrogen production. The method is straightforward, rapid, and efficient for synthesizing a graphite carbon nitride-nickel sulfide system, which holds great promise in the fields of material science and photocatalysis.

Experimental part

Materials

In this work nickel nitrate hexahydrate ($Ni(NO3)_2 \cdot 6H_2O$), sodium sulfide nanohydrate ($Na_2S \cdot 9H_2O$), urea (CH_4N_2O), glycerol ($C_3H_8O_3$), sodium hydroxide (NaOH), sulfur (S) were used. All reagents were analytical grade. Distilled water was used as a solvent.

Synthesis of pristine g – C_3N_4

The g-C_3N_4 was synthesized by calcination of urea in a crucible with a cover in the atmosphere of air. An amount of 30 g of urea was placed in a crucible with a cover and heated to 500 °C for 2 h. After cooling to room temperature, the yellow product was collected and grinded into powder [22].

Synthesis of g-C_3N_4/NiS system

The g-C_3N_4/NiS was prepared through an ion exchange reaction by precipitation method at room temperature. In a typical synthesis, 0,4 g of g-C_3N_4 was dispersed in 25mL of distilled water by ultrasonication for 15 minutes and then, 2 mL of 0.1M $Ni(NO_3)_2$ solution was poured drop by drop in the g-C_3N_4 dispersion. After stirring for 20 min, 2 mL of 0.1M Na_2S solution was dropwise added. The mixed solution was stirred for another 5 min, collected by centrifuge, and washed with distilled water. Finally, the washed precipitates were dried at 70°C for 24 h [22].

Synthesis of sodium polysulfide Na_2S_n

In a three-necked round bottom flask with a reflux condenser, a 100 ml solution of NaOH, with a concentration of 1,25M was poured. Then, 5,33 g of grinded sulfur was added to get Na_2S_2. The dispersed mixture was constantly stirred and heated to 96°C, with a heating rate of 10 °C/min, and kept at this temperature for 15 minutes. The chemical reaction (1) of polysulfide formation is given bellow [23]:

$$6NaOH+6S=2Na_2S_2+Na_2S_2O_3+H_2O \quad (1)$$

Synthesis of g-C_3N_4/NiS_2 system

In a typical synthesis, 0.4 g of g-C_3N_4 was dispersed in 25 mL of distilled water by ultrasonication for 15 minutes and then 2 mL of 0.1M of $Ni(NO_3)_2$ solution was dropwise added in the g-C_3N_4 dispersion. After stirring for 20 minutes, 0,1 mL of Na_2S_2 solution was added to the resulting solution. The mixed solution was stirred for another 5 min, collected by centrifuge, and washed with distilled water three times. Finally, the washed precipitates were dried at 70°C for 24 h.

The final composition of double systems was the next: 99,25 wt% of the g-C_3N_4 and 0.75 wt% of the NiS or NiS_2. These solid powders were subsequently used for further investigation through physicochemical analytical methods.

Characterization

XRD analysis was performed using a MiniFlex 600 diffractometer (Rigaku, Japan) with the following parameters: X-ray tube current of 15 mA, tube voltage of 40 kV, point intensity measurement time of 0,12 seconds, and a goniometer step size of 0,02° 2θ. During the measurement, the sample was rotated at 60 rpm. The ICCD-PDF2 Release 2016 database and PDXL2 software were used to identify phase composition. FT-IR spectra were obtained with the help of Nicolet iS-10 spectrometer (Thermo Fisher Scientific, USA), in the wavelength range 4000 – 450 cm^{-1}. Scanning electron microscopy (SEM) was employed to examine the morphology and particle size of the samples, utilizing an SEM Quanta 3D 200i instrument (FEI, Netherlands). The samples

were attached to a conducting carbon adhesive tape substrate. A JEOL JEM-2100 transmission electron microscope (Japan) operating at 200 kV with an Oxford Instruments X-Max energy-dispersive X-ray spectroscopy detector (UK) was used to perform fine microstructural studies.

Photocatalytic H_2 *Production*

In a typical experiment, 10 mL of glycerol and 90 mL of distilled water were added to 30 mg of the photocatalyst. The solution was stirred to ensure uniform irradiation of the photocatalyst dispersion. Photocatalytic H_2 production occurred in a three-neck round-bottom flask reactor with external irradiation, using a 300 W Xe lamp as the light source and a UV-cut filter (λ > 400 nm).To remove dissolved oxygen, the solution was bubbled with argon for 60 minutes in the dark. The light intensity in the photocatalytic reactor was 30 mW/cm². The reactor was connected to an argon (Ar) stream (312 mL/min), which was used to transport H_2 from the photoreactor to the gas chromatograph (Chromos GCh-100, Russia). Hydrogen concentration measurements were taken every 15 minutes after initiating photocatalyst irradiation [24]. The hydrogen evolution rate (HER) was determined by considering the flow rate of the outgoing gas, the volumetric concentration of hydrogen, and the laboratory's temperature and pressure. This approach facilitated the calculation of the amount of hydrogen that could be reduced on the surface of 1 g of photocatalyst per hour under the given conditions. The volumetric concentration of hydrogen and subsequent HER calculations were performed three times. To ensure the accuracy of the obtained data, statistical analysis was conducted using the standard deviation (SD) (1) [25]:

$$SD = \sqrt{\frac{\sum (X - X_{mean})^2}{n - 1}} \quad (1)$$

X is individual number of HER, X_{mean} is HER mean, n is sample size.

Results and discussion

XRD analysis

The XRD analysis was used to analyze the structure of the synthesized photocatalysts. Figure 1 displays the XRD patterns of the g-C_3N_4/NiS, g-C_3N_4/NiS_2, and pristine materials. The g-C_3N_4, g-C_3N_4/NiS, and g-C_3N_4/NiS_2 XRD spectra are represented by distinct diffraction peaks at 27,46° which can be indexed for graphitic materials as the (100) peak of PDF card No.: 00-066-0813. However, the peak at 12,93° was not identified for double systems, which means that the graphitic-layered structure was changed for these samples. Moreover, the absence of nickel sulfide diffraction peaks is attributed to their deformed amorphous crystal lattice, which complicates their identification using XRD [26].

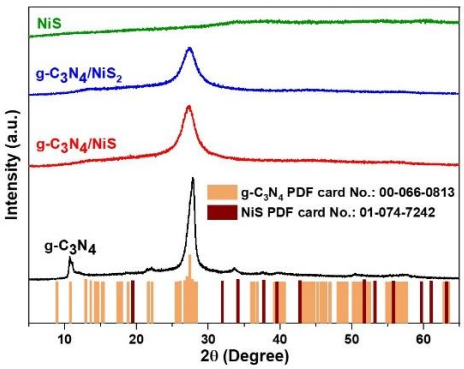

Figure 1 – XRD patterns for composites g-C_3N_4/NiS, g-C_3N_4/NiS_2 and for pristine NiS, g-C_3N_4

FT-IR spectroscopy

In order to analyze the surface groups of the synthesized samples, FT-IR spectroscopy was conducted. In Figure 2, peaks ranging between 1200 and 1700 cm^{-1} indicate the stretching of aromatic heptazine-derived repeating units, manifesting typical sp^2 C═N stretching modes and out-of-plane bending of the sp^3 C−N bonds [27, 28]. Additionally, the absorption peak at 809 cm^{-1} corresponds to the characteristic breathing of tri-s-triazine cycles and the deformation mode of N−H in amino groups, respectively.

A peak at 2178 cm-1 corresponds to the C ═ N bond [29]. The absorption peak at 1618 cm^{-1} is assigned to the vibration of O–H bonds indicating the presence of adsorbed molecules of H_2O. While the peak at 605 cm^{-1} can be probably related to Ni-S stretching vibration mode [30]; this low-intensity peak is visible for bare NiS, while for double systems this stretching vibration mode was not detected. The absorption peaks for g-C_3N_4 are more intense compared to nickel sulfide, due to its lower content, resulting in overlap with each other.

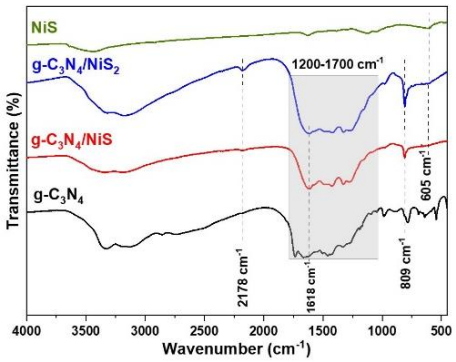

Figure 2 – FT-IR spectra for composites g-C_3N_4/NiS, g-C_3N_4/NiS_2, g-C_3N_4/NiS_3 and g-C_3N_4/NiS_4 and for pure NiS, g-C_3N_4.

SEM

SEM analysis was conducted for the investigation of the morphology and particle size of synthesized samples. The results of analysis for g-C_3N_4, NiS, g-C_3N_4/NiS, and g-C_3N_4/NiS_2 are depicted in Figure 3 a-d. As can be seen, g-C_3N_4, g-C_3N_4/NiS and g-C_3N_4/NiS_2 (Figure 3 a, c, d) samples has a heterogeneous system, the stacked flat sheets with wrinkles and an irregular shape morphology and rough surface. There is also the presence of irregular-shaped pores visible. As for NiS (Figure 3 b), the material is represented by nanosized particles of spherical shape, which form big agglomerates. However, the presence of NiS particles was difficult to identify on the surface of double systems with g-C_3N_4, due to the small amount of metal sulfide in the composition.

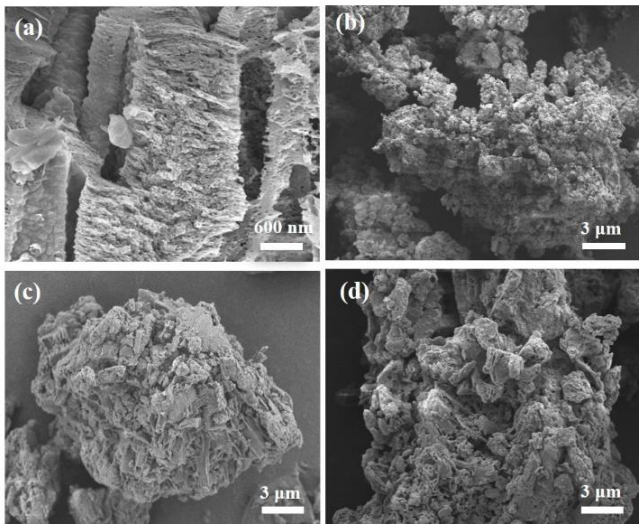

Figure 3 – SEM images of the (a) g-C_3N_4, (b) NiS, (c) g-C_3N_4/NiS and (c) g-C_3N_4/NiS_2

TEM and TEM elemental mapping

TEM analysis was conducted for g-C_3N_4/NiS_2 only, for a deeper study of the morphology of the sample. TEM elemental mapping was made to understand the elemental distribution and prove the presence of metal sulfide in the composition. TEM images are given in Figure 4 a, b, where the presence of irregularly curved layers is visible. In addition, the presence of pores with a size of no more than 50 nm is observed on the layers. TEM elemental mapping (Figure 4 c-g) showed the presence of carbon, nitrogen, nickel, and sulfur elements. It can be seen, that nickel and sulfur are uniformly distributed on the surface of g-C_3N_4.

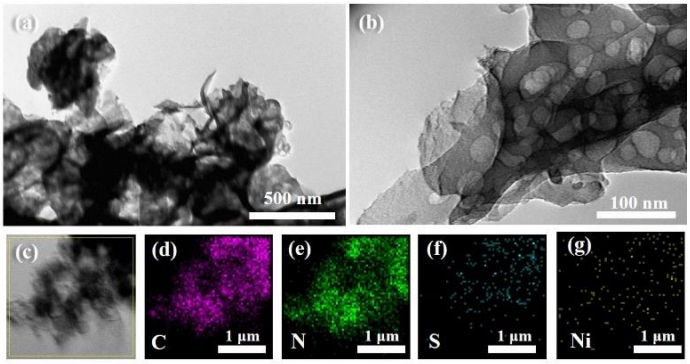

Figure 4 – (a), (b) TEM images of the g-C_3N_4/NiS_2 and EDS mapping image (c) mapping area, (b) carbon, (c) nitrogen, (f) sulfur, (g) nickel

Photocatalytic hydrogen evolution

Synthesized samples were applied for photocatalytic hydrogen production. The activity of the double systems was compared with the bare g-C_3N_4, as the main goal of the study was improving of the photocatalytic activity of this material by adding NiS co-catalyst, with subsequent comparison of the activity of the samples. Bare g-C_3N_4 was not able to produce hydrogen without a co-catalyst. Between double systems, the g-C_3N_4/NiS_2 revealed the highest activity, which slightly increased during the whole photocatalytic process. The gradual increase in the HER throughout the entire period of light irradiation indicates that the sample remained active. This trend suggests that the photocatalyst sustained its functionality without deactivation, continuously facilitating the hydrogen production process under the applied conditions. The highest HER amount of 57,09 $\mu molh^{-1}g^{-1}$ was on the 180th min of visible light irradiation. For g-C_3N_4/NiS, the highest HER was observed at the 135th minute of light irradiation, reaching 32,26 μmol h^{-1} g^{-1}. This value remained constant until the end of the process, indicating that the photocatalyst exhibited stability and maintained a consistent hydrogen production rate throughout the experiment. In general, the application of the NiS and NiS_2 as co-catalysts for g-C_3N_4 revealed prospective results. A hybrid system could provide better results than pure g-C_3N_4. This is possible thanks to a suitable zone structure, which is complemented by the recovery potential of NiS and NiS_2 [19, 20]. Our results are relatively comparable to those presented in [31], where g-C_3N_4/NiS samples with varying compositions were studied. In that study, g-C_3N_4/NiS with 1, 2, 3, 4, and 6% NiS exhibited HER values of 36, 61, 79, 72, and 33 μmol h^{-1} g^{-1}, respectively [31]. However, it is important to note that direct comparisons between results from different publications may not be entirely valid, as experimental conditions vary across studies. Therefore, drawing conclusions about the differences or similarities between these results would be inappropriate.

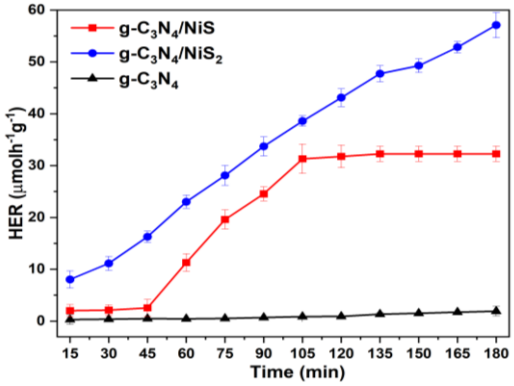

Figure 5 – HER of the prepared samples

Conclusions

The g-C_3N_4/NiS and g-C_3N_4/NiS_2 were prepared through an ion-exchange precipitation method at room temperature.

The XRD and FT-IR showed the presence of g-C_3N_4 for all double systems but did not show the presence of NiS. NiS and NiS_2 are represented by a deformed amorphous crystal lattice, which complicates its identification using XRD. According to SEM results, g-C_3N_4/NiS and g-C_3N_4/NiS_2

samples have heterogeneous systems, stacked flat sheets with wrinkles and an irregular shape morphology and rough surface. The presence of irregularly shaped pores is also noticeable. TEM proved the presence of irregularly curved layers of the g-C_3N_4, while TEM elemental mapping showed the presence of the carbon, nitrogen, sulfur, and nickel elements.

Comparative study of the photocatalytic hydrogen evolution showed, that the best co-catalyst on the surface of g-C_3N_4 was NiS_2 0,75 wt%. The H_2 evolution rate increases as the time of irradiation increases. The highest concentration of hydrogen was reached on the 3rd hour of the visible light irradiation and was equal to 56.79 $\mu molh^{-1}g^{-1}$.

References

1. Ozili P.K., Ozen E. Global Energy Crisis. The Impact of Climate Change and Sustainability Standards on the Insurance Market / P.K. Ozili, E. Ozen // New York: John Wiley & Sons, Ltd. – 2023. – P. 439-454.
2. Marbán G. T. Towards the hydrogen economy?/ G. Marbán, T. Valdés-Solís // International Journal of Hydrogen Energy. – 2007. – Vol. 32, № 12. – P. 1625-1637.
3. Lemus R.G. Updated hydrogen production costs and parities for conventional and renewable technologies / R.G. Lemus, J.M. Martínez Duart // International Journal of Hydrogen Energy. 2010. – Vol. 35, № 9. – P. 3929-3936.
4. Hydrogen production from crude pyrolysis oil by a sequential catalytic process / T. Davidian et al // Applied Catalysis B: Environmental. – 2007. – Vol. 73, № 1. – P. 116-127.
5. A review on biomass-based hydrogen production for renewable energy supply / S.E. Hosseini et al // International Journal of Energy Research. – 2015. – Vol. 39, № 12. – P. 1597-1615.
6. Hydrogen production by photovoltaic-electrolysis using aqueous waste from ornamental stones industries / F.C. Marques et al // Renewable Energy. – 2020. – Vol. 152. – P. 1266-1273.
7. Soluble g-C3N4 nanosheets: Facile synthesis and application in photocatalytic hydrogen evolution / X. Wu et al // Applied Catalysis B: Environmental. – 2019. – Vol. 247. – P. 70-77.
8. Fujishima A. Electrochemical Photolysis of Water at a Semiconductor Electrode / A. Fujishima, K. Honda // Nature. – 1972. – Vol. 238, № 5358. – P. 37-38.
9. Molecular engineering of carbon nitride towards photocatalytic H2 evolution and dye degradation / A. Hayat et al // Journal of Colloid and Interface Science. – 2021. – Vol. 597. – P. 39-47.
10. Enhanced light-driven hydrogen generation in carbon nitride photocatalysts by interfacial electron-transfer cascade / X. Yin et al // Journal of Alloys and Compounds. – 2022. – Vol. 894. – P. 162499.
11. Recent developments in fabrication and structure regulation of visible-light-driven g-C3N4-based photocatalysts towards water purification: A critical review: Advances in photo(electro)catalysis for environmental applications and chemical synthesis / S. Zhang et al // Catalysis Today. – 2019. – Vol. 335. – P. 65-77.
12. A metal-free polymeric photocatalyst for hydrogen production from water under visible light / X. Wang et al // Nature Materials. – 2009. – Vol. 8, № 1. – P. 76-80.
13. Lin L. Crystalline Carbon Nitride Semiconductors for Photocatalytic Water Splitting / L. Lin, Z. Yu, X. Wang // Angewandte Chemie. – 2019. – Vol. 131, №19. – P. 6225-6236.
14. Graphitic carbon nitride (g–C3N4)–based metal-free photocatalysts for water splitting: A review / A. Mishra et al // Carbon. – 2019. – Vol. 149. – P. 693-721.
15. Positioning cyanamide defects in g-C3N4: engineering energy levels and active sites for superior photocatalytic hydrogen evolution / J. Yuan et al // Applied Catalysis B: Environmental. – 2018. – Vol. 237. – P. 24-31.
16. Facile constructing of isotype g-C3N4(bulk)/g-C3N4(nanosheet) heterojunctions through thermal polymerization of single-source glucose-modified melamine: An efficient charge separation system for photocatalytic hydrogen production / S. Sun et al // Applied Surface Science. – 2020. – Vol. 500. – P. 143985.
17. Critical roles of co-catalysts for molecular hydrogen formation in photocatalysis / Y.H. Li et al // Journal of Catalysis. – 2015. – Vol. 330. – P. 120-128.
18. Low Metal Loading (Au, Ag, Pt, Pd) Photo-Catalysts Supported on TiO2 for Renewable Processes / F. Conte et al // Materials. – 2022. – Vol. 15, № 8. – P. 2915.
19. NiS2 Co-catalyst decoration on CdLa2S4 nanocrystals for efficient photocatalytic hydrogen generation under visible light irradiation / Y.-P. Yuan et al // International Journal of Hydrogen Energy. – 2013. – Vol. 38, № 18. – P. 7218-7223.

20. CuS, NiS as co-catalyst for enhanced photocatalytic hydrogen evolution over TiO2 / Q. Wang et al // International Journal of Hydrogen Energy. – 2014. – Vol. 39, № 25. – P. 13421-13428.
21. Carbonized MoS2: Super-active co-catalyst for highly efficient water splitting on CdS / M. Shao // ACS Sustainable Chemistry & Engineering. – 2019. – Vol. 7, № 4. – P. 4220-4229.
22. NiS and graphene as dual cocatalysts for the enhanced photocatalytic H 2 production activity of g-C 3 N 4 / Z. Chen et al // Applied Surface Science. – 2019. – Vol. 469. – P. 657-665.
23. Khusainov A.N. Physico-chemical patterns of formation of sulfur nanoparticles obtained by grinding and chemical deposition methods [The electron.source] / A.N. Khusainov. – 2015. URL: https://rusneb.ru/catalog/000199_000009_008040370/ (Date of appeal 27.09.2024) (In Russian).
24. Heterostructured g-cn/tio2 photocatalysts prepared by thermolysis of g-cn/mil-125(Ti) composites for efficient pollutant degradation and hydrogen production / B. Tatykayev et al // Nanomaterials. – 2020. – Vol. 10, № 7. – P. 1-19.
25. Barde M.P. What to use to express the variability of data: Standard deviation or standard error of mean? / M.P. Barde, P.J. Barde // Perspectives in clinical research. – 2012. – № 3, Vol. 3. – P. 113-116.
26. The Synergistic Effect of MoS2 and NiS on the Electrical Properties of Iron Anodes for Ni-Fe Batteries / H. Tang et al // Nanomaterials. – 2022. – Vol. 12, № 19. – P. 3472.
27. Constructing Multifunctional Metallic Ni Interface Layers in the g-C3N4 Nanosheets/Amorphous NiS Heterojunctions for Efficient Photocatalytic H2 Generation / J. Wen et al // ACS applied materials & interfaces. – 2017. – Vol. 9.
28. Enhanced visible light photocatalytic activity and oxidation ability of porous graphene-like g-C3N4 nanosheets via thermal exfoliation / F. Dong et al // Applied Surface Science. – 2015. – P. 358.
29. In Situ Polycondensation Synthesis of NiS-g-C3N4 Nanocomposites for Catalytic Hydrogen Generation from NaBH4 / A.H. Alshammari et al // Nanomaterials. – 2023. – Vol. 13, № 5. – P. 938.
30. Electrochemical performance of β-Nis@ Ni (OH) 2 nanocomposite for water splitting applications / B. Jansi Rani et al // ACS omega. – Vol. 4, № 6. – P.10302-10310.
31. NiS and graphene as dual cocatalysts for the enhanced photocatalytic H2 production activity of g-C3N4 / Z. Chen et al // Applied Surface Science. – 2019. – № 469. – P. 657-665.

Acknowledgments

This research was funded by the Science Committee of the Ministry of Education and Science of the Republic of Kazakhstan (Grant № AP13068426).

Н. Мақсұт, Б. Татыкаев, С. Түгелбай, А. Әбілхан, Н. Хан[2*]
[1]Әл-Фараби атындағы Қазақ Ұлттық Университеті,
050040, Қазақстан, Алматы, Әл-Фараби даңғылы 71
[2]Назарбаев, Университеті,
010000, Қазақстан, Астана, Қабанбай батыр даңғылы 53,
*e-mail: natalya.khan@nu.edu.kz

СУТЕГІНІ ФОТОКАТАЛИТИКАЛЫҚ ӘДІСПЕН ӨНДІРУ ҮШІН NIS ЖӘНЕ NIS_2 КО-КАТАЛИЗАТОРЛАРЫН ИОН АЛМАСУ РЕАКЦИЯСЫ АРҚЫЛЫ G-C_3N_4 БЕТІНЕ ДЕКОРАТИВТІ ОТЫРҒЫЗУҒА АРНАЛҒАН САЛЫСТЫРМАЛЫ ЗЕРТТЕУ ЖҰМЫСЫ

NiS және NiS2 со-катализаторларды g-C3N4 бетіне ион алмасу реакциясы арқылы тұндыру әдісімен декорланды. Синтезделген қос жүйелер РФТ, ИҚ спектроскопиясы, СЭМ, ПЭМ және ПЭМ-элементтік карталау арқылы зерттелді. РФТ және ИҚ спектроскопиясы g-C3N4/NiS және g-C3N4/NiS2 құрамында g-C3N4 бар екенін көрсетті, алайда никель сульфидтерінің бар екендігі анықталған жоқ. СЭМ талдау қос жүйелердің гетерогенді құрылымға ие екенін, қабаттардың бір-бірінің үстіне орналасқанын және бөлшектердің морфологиясы түзілмеген пішінде және кедір-бұдырлы бетті екенін көрсетті. ПЭМ талдауы g-C3N4 қабаттарының түзілмеген пішінді екенін дәлелдеді, ал ПЭМ элементтік карталау азот, көміртек, күкірт және никельдің бар екенін көрсетті. Синтезделген үлгілердің фотокаталитикалық сутегін бөлу зерттеулері g-C3N4/NiS2-нің g-C3N4/NiS және g-C3N4-ке қарағанда ең жоғары сутегі бөлу жылдамдығын ие екенін көрсетті. Осылайша, ең жоғары сутегінің жылдамдық бөлуі 56,79 μмоль/сағ-1г-1 құрайтын g-C3N4/NiS2 композитін 3 сағат көрінетін жарықпен сәулеленгенінде қол жеткізілді.

Түйін сөздер: *графитті көміртек нитриді, никель сульфиді, со-катализатор, фотокатализатор, сутегін бөлу.*

Н. Мақсұт, Б. Татыкаев, С. Түгелбай, А. Абилхан, Н. Хан[2*]
[1]Казахский национальный университет им. аль-Фараби,
050040, Республика Казахстан, г. Алматы, пр. аль-Фараби, 71
[2]Назарбаев Университет,
010000, Республика Казахстан, г. Астана, пр. Кабанбай батыра, 53
*e-mail: natalya.khan@nu.edu.kz

СРАВНИТЕЛЬНОЕ ИССЛЕДОВАНИЕ ФОТОКАТАЛИТИЧЕСКОГО ВЫДЕЛЕНИЯ ВОДОРОДА ПРИ ПОМОЩИ G-C_3N_4, ДЕКОРИРОВАННОГО СО-КАТАЛИЗАТОРАМИ NIS И NIS_2 МЕТОДОМ ИОНООБМЕННОГО ОСАЖДЕНИЯ

Со-катализаторы NiS и NiS_2 были декорированы на поверхность g-C_3N_4 посредством реакции ионного обмена методом осаждения. Синтезированные двойные системы были исследованы с помощью РФА, ИК спектроскопии, СЭМ, ПЭМ и ПЭМ-элементного картирования. РФА и ИК спектроскопия показали присутствие g-C_3N_4 в составе g-C_3N_4/NiS и g-C_3N_4/NiS_2, однако присутствие сульфидов никеля обнаружено не было. СЭМ-анализ показал, что двойные системы имеют неоднородную структуру, плоские слои, наложенные друг на друга, а морфолоигя частиц представлена неправильной формой и шероховатой поверхностью. ПЭМ доказала наличие слоев g-C_3N_4 неправильной формы, а элементное картирование ПЭМ показало наличие азота, углерода, серы и никеля. Исследование фотокаталитического выделения водорода синтезированными образцами показало, что g-C_3N_4/NiS_2 проявляет самую высокую скорость выделения водорода по сравнению с g-C_3N_4/NiS и g-C_3N_4. Таким образом, наибольшая скорость выделения водорода была достигнута для g-C_3N_4/NiS_2 на 3-м часу облучения видимым светом, которая составила 56,79 μмоль/ч$^{-1}$г$^{-1}$.

Ключевые слова: *графитовый нитрид углерода, сульфид никеля, со-катализатор, фотокатализатор, выделение водорода.*

Information about the authors

Nazgul Maksut – MSc, Junior researcher of the Department of General and Inorganic Chemistry, Al-Farabi Kazakh National University, Almaty, Kazakhstan; e-mail: Maksut-n@mail.ru.

Batukhan Tatykayev – PhD, Leading researcher of the Laboratory of Advanced Materials and Systems for Energy Storage, PI «National Laboratory Astana», Astana, Kazakhstan; e-mail: batukhan.tatykayev@nu.edu.kz. ORCID: https://orcid.org/0000-0001-5071-1968.

Saparbek Tugelbay – MSc, Researcher of the Laboratory of Advanced Materials and Systems for Energy Storage, PI «National Laboratory Astana», Astana, Kazakhstan; e-mail: saparbek.tugelbay@nu.edu.kz. ORCID: https://orcid.org/0000-0002-8781-9320.

Abylay Abilkhan – MSc, Researcher of the Laboratory of Advanced Materials and Systems for Energy Storage, PI «National Laboratory Astana», Astana, Kazakhstan; e-mail: abylay.abilkhan@nu.edu.kz. ORCID: https://orcid.org/0000-0003-1227-5004.

Natalya Khan* – PhD, Researcher of the Laboratory of Advanced Materials and Systems for Energy Storage, PI «National Laboratory Astana», Astana, Kazakhstan; e-mail: natalya.khan@nu.edu.kz. ORCID: https://orcid.org/0000-0003-1794-0018.

Авторлар туралы мәліметтер

Назгүл Мақсұт – MSc, Әл-Фараби атындағы Қазақ Ұлттық Университеті, Химия және химиялық технология факультеті, Жалпы және бейорганикалық химия кафедрасының кіші ғылыми қызметкері, Алматы, Қазақстан; e-mail: Maksut-n@mail.ru.

Батухан Татыкаев – PhD, «National Laboratory Astana» ЖМ жетекші ғылыми қызметкері, Астана, Қазақстан; e-mail: batukhan.tatykayev@nu.edu.kz. ORCID: https://orcid.org/0000-0001-5071-1968.

Сапарбек Түгелбай – MSc, «National Laboratory Astana» ЖМ, Жаңа материалдар және энергияны сақтау жүйелері зертханасының ғылыми қызметкері, Астана, Қазақстан; e-mail: saparbek.tugelbay@nu.edu.kz. ORCID: https://orcid.org/0000-0002-8781-9320.

Абылай Әбілхан – MSc, «National Laboratory Astana» ЖМ, Жаңа материалдар және энергияны сақтау жүйелері зертханасының ғылыми қызметкері, Астана, Қазақстан; e-mail: abylay.abilkhan@nu.edu.kz. ORCID: https://orcid.org/0000-0003-1227-5004.

Наталья Хан* – PhD, «National Laboratory Astana» ЖМ, Жаңа материалдар және энергияны сақтау жүйелері зертханасының ғылыми қызметкері, Астана, Қазақстан; e-mail: natalya.khan@nu.edu.kz. ORCID: https://orcid.org/0000-0003-1794-0018.

Сведения об авторах

Назгүл Мақсұт – MSc, Младший научный сотрудник кафедры Общей и неорганической химии, КазНУ им. Аль-Фараби, Алматы, Казахстан; e-mail: Maksut-n@mail.ru.

Батухан Татыкаев – PhD, Ведущий научный сотрудник ЧУ «National Laboratory Astana», Астана, Казахстан; e-mail: batukhan.tatykayev@nu.edu.kz. ORCID: https://orcid.org/0000-0001-5071-1968.

Сапарбек Түгелбай – MSc, Научный сотрудник Лаборатории новых материалов и систем хранения энергии, ЧУ «National Laboratory Astana», Астана, Казахстан, e-mail: saparbek.tugelbay@nu.edu.kz. ORCID: https://orcid.org/0000-0002-8781-9320.
Абылай Әбілхан – MSc, Научный сотрудник Лаборатории новых материалов и систем хранения энергии, ЧУ «National Laboratory Astana», Астана, Казахстан; e-mail: abylay.abilkhan@nu.edu.kz. ORCID: https://orcid.org/0000-0003-1227-5004.
Наталья Хан* – PhD, Научный сотрудник Лаборатории новых материалов и систем хранения энергии, ЧУ «National Laboratory Astana», Астана, Казахстан; e-mail: natalya.khan@nu.edu.kz. ORCID: https://orcid.org/0000-0003-1794-0018.

Received 03.10.2024
Revised 19.11.2024
Accepted 20.11.2024

https://doi.org/10.53360/2788-7995-2024-4(16)-45

IRSTI: 55.22.19

M. Maulet*, Zh.B. Sagdoldina[1,2], A. Çoruh [3], A.B. Alibekova[1]
[1]Sarsen Amanzholov East Kazakhstan University,
070002, Kazakhstan, Ust-Kamenogorsk, st. Shakarima 148
[2]Shakarim University of Semey,
071412, Kazakhstan, Semey, st. Glinka, 20 A
[3]Sakarya University,
54050, Turkey, Sakarya, Esentepe
*e-mail: maulet_meruert@mail.ru

INVESTIGATION OF TRIBOLOGICAL PROPERTIES OF DETONATION Ni-Cr-Al COATINGS

This study explores the tribological properties of Ni-Cr-Al coatings applied through detonation spraying technology, with a focus on the comparison between gradient coatings and homogeneous coatings. Ni-Cr-Al coatings, widely used in aerospace, automotive, and energy industries like power plants, are valued for their exceptional hardness, wear resistance, and high-temperature stability. Gradient coatings, produced by tailoring the detonation spraying parameters, exhibit a microstructure combining a hard, wear-resistant surface with a softer, ductile subsurface, enhancing their load-bearing capacity and tribological performance. Experimental results reveal that gradient coatings achieve lower and more stable friction coefficients (0.3-0.4) compared to homogeneous coatings (0,4-0,5), attributed to their optimized stress distribution and reduced adhesive interactions. These findings underscore the superior wear resistance and durability of gradient Ni-Cr-Al coatings, making them highly suitable for applications involving prolonged operation under sliding conditions. This research contributes to the development of advanced coating systems optimized for demanding operational environments.

Key words: *detonation spraying, Ni-Cr-Al coatings, gradient coatings, homogeneous coatings, tribological properties.*

Introduction

High-performance coatings are essential for enhancing the durability and efficiency of engineering components, especially those exposed to extreme mechanical and thermal stresses. Among various coating systems, nickel-chromium-aluminum (Ni-Cr-Al) coatings have garnered significant attention due to their excellent combination of hardness, corrosion resistance, and high-temperature stability. These properties make Ni-Cr-Al coatings ideal for applications in aerospace, automotive, and energy sectors [1-2]. Detonation spraying is a thermal spray technique that effectively deposits Ni-Cr-Al coatings. Studies have shown that the degree to which the detonation gun barrel is filled with the gas mixture significantly influences the chemical composition and phase structure of the resulting coatings. For instance, higher filling degrees can decrease aluminum content, affecting the formation of Ni-Al phases, which are crucial for enhancing wear resistance [3-4].